

Lawrence Berkeley National Laboratory

Recent Work

Title

PHOTOPHYSICAL AND PHOTOCHEMICAL ASPECTS OF THE BINDING OF ZINC PORPHYRIN TO SODIUM POLY (STYRENE SULFONATE)

Permalink

<https://escholarship.org/uc/item/41z863gh>

Author

Goswami, K.

Publication Date

1987-08-01



Lawrence Berkeley Laboratory

UNIVERSITY OF CALIFORNIA

CHEMICAL BIODYNAMICS DIVISION

Submitted to Journal of the American Chemical Society

**Photophysical and Photochemical Aspects of the Binding
of Zinc Porphyrin to Sodium Poly(styrene sulfonate)**

K. Goswami, T.E. Casti, J.W. Otvos, and M. Calvin

August 1987

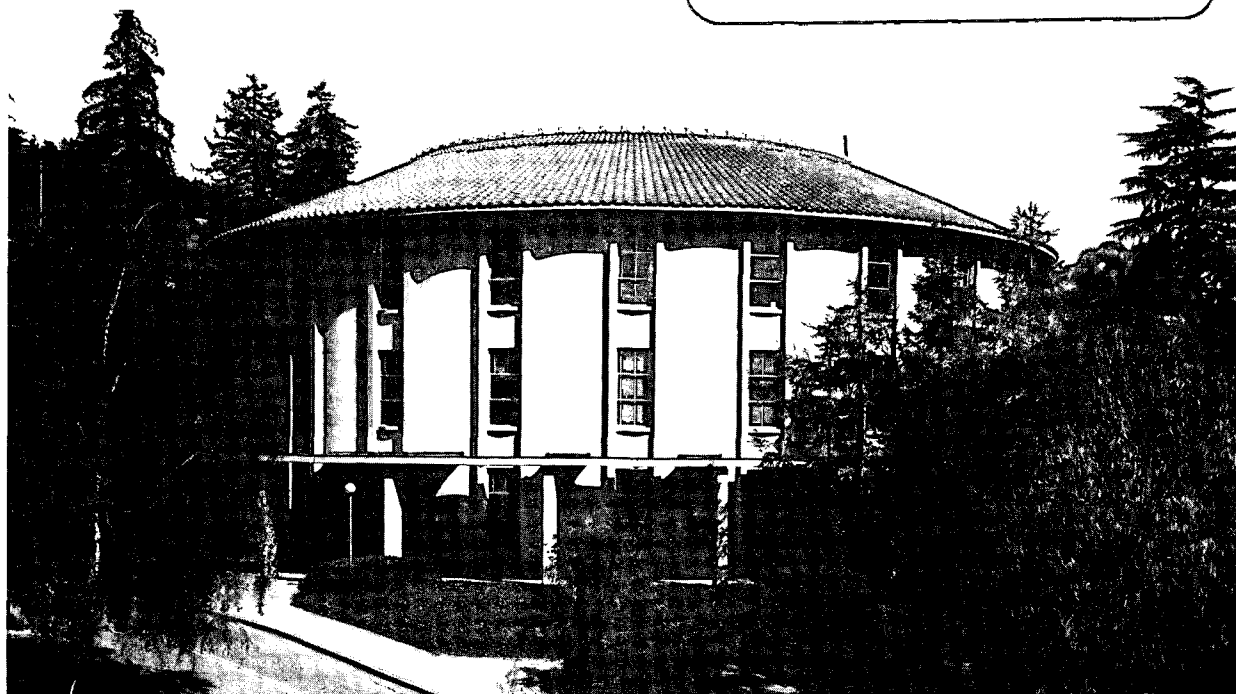
RECEIVED
LAWRENCE
BERKELEY LABORATORY

OCT 19 1987

LIBRARY AND
DOCUMENTS SECTION

For Reference

Not to be taken from this room



DISCLAIMER

This document was prepared as an account of work sponsored by the United States Government. While this document is believed to contain correct information, neither the United States Government nor any agency thereof, nor the Regents of the University of California, nor any of their employees, makes any warranty, express or implied, or assumes any legal responsibility for the accuracy, completeness, or usefulness of any information, apparatus, product, or process disclosed, or represents that its use would not infringe privately owned rights. Reference herein to any specific commercial product, process, or service by its trade name, trademark, manufacturer, or otherwise, does not necessarily constitute or imply its endorsement, recommendation, or favoring by the United States Government or any agency thereof, or the Regents of the University of California. The views and opinions of authors expressed herein do not necessarily state or reflect those of the United States Government or any agency thereof or the Regents of the University of California.

PHOTOPHYSICAL AND PHOTOCHEMICAL ASPECTS OF THE BINDING OF ZINC PORPHYRIN TO SODIUM POLY(STYRENE SULFONATE)

Kisholoy Goswami, Thomas E. Casti, John W. Otvos and Melvin Calvin

*Lawrence Berkeley Laboratory and Department of Chemistry
University of California, Berkeley, CA 94720, U. S. A.*

Abstract

By laser flash and steady state techniques we have explored the effect of the polyelectrolyte sodium poly(styrene sulfonate) (PSS) on the photoinduced electron transfer reaction between zinc(II) tetrakis(4-N-methylpyridinium)porphyrin (ZnP^{4+}) and propyl viologen sulfonate (PVS). We have found that the photophysical and photochemical properties of ZnP^{4+} depend on the molecular weight of PSS and on the P/D ratios, where, P = molar concentration of the sulfonate groups on PSS and D = molar concentration of ZnP^{4+} . With the addition of PSS, the overall absorption intensity of the Soret band first decreases and then increases with a simultaneous red-shift in the maximum. The overall emission intensity also first decreases with the addition of PSS and then increases with a blue-shift in the maximum. These absorption and emission features have been ascribed to the aggregation of ZnP^{4+} species on the polyelectrolyte molecules and to the environmental influence of PSS. PSS of molecular weight 500,000 shows a more dramatic influence on the properties of ZnP^{4+} than the 4,000 molecular weight one. With triethanolamine as a sacrificial donor the quantum yield of $PVS^{\bullet-}$ radical formation increases upon the addition of a large excess of PSS. Laser flash experiments in the absence of sacrificial donor show that PSS (4k, P/D = 25) retards the rate of back electron transfer (k_b) by three orders of magnitude compared to the rate in pure water. However, the forward electron transfer rate (k_f) is diminished by a factor of 25. The decrease in the reverse electron transfer rate is attributed to the electrostatic interaction between PSS and the photoproducts. The decrease in k_f is explained by the hydrophobic encapsulation of ZnP^{4+} by PSS, whereby the bimolecular approach of the two reacting partners is hindered.

There has been a great surge of interest in photoinduced electron transfer reactions in recent years, one driving force being the chemical conversion and storage of solar quanta. However, for the efficient separation of the photogenerated ion pairs (or radicals) the well recognized problem of back electron transfer has always been a limiting factor. Microenvironmental effects of micelles, vesicles, colloids and polyelectrolytes have been employed for the kinetic control of the forward and reverse electron transfer steps¹⁻¹⁰ and moderate success has been achieved. Among these structural assemblies, polyelectrolytes often offer a very attractive choice because of their electrostatic, hydrophobic and hydrophilic characteristics.^{6,8,11,12} Also, they provide a relatively rigid extended structure along which photogenerated charges in the bound species may travel.

In the studies concerning interfacial photochemistry based on interaction of the counter ions with polyelectrolytes, emphasis should be placed on such parameters as chain length and P/D ratio, where P = bulk concentration of the equivalent monomer residue and D = concentration of donor or acceptor species (dye)* so that the environmental effect exerted by polyelectrolytes can be fully appreciated. These parameters indeed play a critical role in modifying photophysical properties.¹³

In an earlier publication from this group,⁴ the effect of the polyelectrolyte, sodium poly(styrene sulfonate) (PSS, molecular weight = 4,000; P/D \approx 200), on the photoinduced electron transfer reaction between zinc(II) tetrakis(4-N-methylpyridinium)porphyrin (ZnP^{4+}) and propyl viologen sulfonate (PVS) has been reported. By flash photolysis studies, it was shown that PSS significantly decreases the reverse and also the forward electron transfer rates. By steady state and flash photolysis techniques, we have extended this study and have made systematic measurements on the effects of P/D ratio and polymer

* Although the term P/D may appear to be artificial, we are using it in order to keep conformity with dye-polymer binding literature.

molecular weight on both the photophysical and photochemical properties of the system. The complete report follows.

Materials:

Zinc(II) tetrakis(4-N-methylpyridinium)porphyrin, chloride salt (ZnP^{4+}) of ultra high purity was purchased from Midcentury. Its absorption and emission properties matched very well with previous work⁴ and therefore it was used without further treatment. Propyl viologen sulfonate (PVS) was prepared as reported before.⁴ Samples of poly(styrene sulfonate, sodium salt) (PSS) of different molecular weights were purchased from Polysciences, Inc. and they were used without additional treatment. Triethanolamine (TEOA, Baker Analyzed Reagent) was used as obtained. Water was distilled and purified by a Millipore Milli-Q system before use.

Methods:

Absorbance measurements were done using a Hewlett-Packard 8450 A uv/vis spectrophotometer. Emission spectra were recorded on a Perkin - Elmer MPF 2A spectrofluorimeter. All absorption and emission experiments were done with quartz cells, 1 cm x 1 cm, employing a 3 ml portion of 5×10^{-6} M air saturated ZnP^{4+} solution. Fluorescence quantum yields were estimated relative to rhodamine B¹⁴ with SPEX Industries' Fluorolog 212T system using the optically dilute method.¹⁵ The spectra were fully corrected for the instrumental response. The fluorescence lifetimes were measured by single photon counting techniques. The medium pH was adjusted with 1M NaOH solution. All absorption and emission measurements were done at room temperature.

Steady state photolyses were done using long neck pyrex cells. Typically, a 3 ml solution containing ZnP^{4+} (1×10^{-5} M), PVS (0.01 M), TEOA (0.10 M) and PSS at pH

10 was rigorously purged with pure argon for 30 mins before photolysis. Simultaneous irradiation and spectrophotometric measurements of the photoproducts were accomplished through the use of a specially designed thermostated cell holder with home made accessories for magnetic stirring of the cell contents. Irradiation of the samples were done by a 450 W Xe lamp. The beam was directed through a fiber optic illumination system containing a 440 nm narrow band pass interference filter. The incident photon flux was determined by ferrioxalate actinometry.¹⁶ Values of $\Phi_{PVS^{\bullet-}}$ were computed from the initial linear formation of the $PVS^{\bullet-}$ radical as a function of irradiation time. Concentration of $PVS^{\bullet-}$ was determined from the absorbance of the photolyzed solution at 600 nm, taking $\epsilon_{600} = 1.28 \times 10^4 \text{ M}^{-1} \text{ cm}^{-1}$.⁴

Triplet lifetimes of ZnP^{4+} and the decay of $PVS^{\bullet-}$ radicals were measured by flash photolysis experiments. Long neck, 1 cm path length pyrex cells were used. Typically, 3 ml solution containing ZnP^{4+} ($1 \times 10^{-5} \text{ M}$), PVS (0.01 M) and PSS ($0 - 2.0 \times 10^{-3} \text{ eq./l}$) was purged with argon for 30 mins before the flash experiment. Laser pulses from a Candela SLL - 66A flash lamp pumped dye laser with output at 590 nm having 100 mJ pulse energy and 200 ns duration were used for the flash studies. Transient absorbance changes for $^3ZnP^{4+}$ and $PVS^{\bullet-}$ were monitored at 480 nm and 600 nm respectively.

Results:

An aqueous solution of ZnP^{4+} exhibits visible absorption bands at 434 nm, the Soret band, and 560 nm as shown in Figure 1. Excitation at either one of the bands leads to singlet emission with a maximum at 630 nm and a shoulder around 660 nm as depicted in Figure 2. The fluorescence quantum yield, independent of the excitation wavelength, is estimated to be ~ 0.03 . From the cross over point of the excitation and emission spectra at 592 nm, the first excited singlet energy is computed to be 202 kJ/mole. The radiative lifetime of the first excited singlet in pure water has been determined by single photon counting techniques and has been found to be 1.4 ns monitoring at both 630 nm and 660 nm.

However, the spectroscopic characteristics of ZnP^{4+} are modified upon the addition of PSS. As PSS of molecular weight 4,000 is added, the intensity of ZnP^{4+} absorption at 434 nm decreases and the λ_{max} shifts to the red. This decrease is greatest, about 10% of the initial absorbance, at $P/D = 4$, where P is the concentration of the monomer residues, i.e., sulfonate groups, and D is the concentration of ZnP^{4+} . At this value of P/D (4), the λ_{max} is at 438 nm as illustrated in Figure 3. With the further addition of PSS, the overall absorbance increases with a progressive red-shift in the λ_{max} up to a high value of 442 nm at $P/D = 25$. Interesting behavior is observed for PSS of molecular weight 500,000. With the addition of this PSS, the absorbance at 434 nm decreases initially, as before, along with slight red-shift of the maximum to 438 nm as shown in Figure 4. However, an additional feature in the absorption spectra is observed in the low P/D regime. At $P/D \leq 3.5$, the absorbance in the region of 448 nm to 550 nm increases as illustrated in Figure 4. The difference spectrum in this region shows the growth of a broad absorption band with maximum at 468 nm. This feature arises from dye-dye interactions when a large number of ZnP^{4+} cations are bound to a single macromolecule. With increasing

P/D ratio, the overall absorbance grows back very slowly unlike with the 4,000 molecular weight PSS as shown in Figure 5. At P/D = 25, with this high molecular weight PSS, the absorbance of ZnP^{4+} , is only $\sim 60\%$ of that without PSS.

The emission properties of ZnP^{4+} are also modified with the addition of PSS. Unlike the absorption maxima, as PSS is added to the medium, the emission maxima undergoes a progressive blue-shift. With PSS of molecular weight 4,000, at P/D = 4, the λ_{em}^{max} is at 625 nm and at P/D ≥ 25 , the λ_{em}^{max} is at 623 nm as shown in Figure 6. For PSS of molecular weight 500,000, the emission intensity is drastically reduced at P/D ≈ 3.5 as shown in Figure 6. At P/D = 25, with this PSS sample, the emission peak appears at 625 nm, however, the intensity is less than that observed with PSS of molecular weight 4,000 as Figure 6 depicts. The spectral characteristics of ZnP^{4+} in the presence of PSS are summarized in Table 1. These changes in the absorption and emission properties arise because of binding interactions of ZnP^{4+} with PSS as explained in the discussion section. The unusual decrease of the emission quantum yield at P/D ≤ 3.5 with PSS of molecular weight 500,000, as Table 1 shows, can be ascribed to dye-dye interaction.¹⁷ The decay profile of the singlet emission at 630 nm shows two components; the major component (60%) having a lifetime of 0.5 ns and the minor (40%) component having a lifetime of 1.4 ns.

With the expectation that the anionic polyelectrolyte, PSS, would enhance the radical yield by selectively repelling $\text{PVS}^{-\bullet}$, we studied the photoinduced electron transfer reaction between ZnP^{4+} (10^{-5}M) and PVS (0.01 M) by steady state photolysis using TEOA (0.10 M) as the sacrificial donor at pH 10. The results given in Table 2 show that the overall quantum yield has a complicated dependence on the chainlength of PSS and P/D ratios. At low P/D ratio, the quantum yield of $\text{PVS}^{-\bullet}$ is less than that in PSS free medium. However, at high P/D ratio, the quantum yield is increased.

Flash photolysis experiments were performed to determine the influence of PSS on the rates of disappearance of ${}^3\text{ZnP}^{4+*}$, monitored at 480 nm and $\text{PVS}^{-\bullet}$ monitored at 600 nm. In the flash experiments, involving ZnP^{4+} and PVS, no sacrificial electron donor was added. The only reaction of the primary electron transfer products is the back reaction with one another. The reverse electron transfer rate (k_b) was deduced by fitting the decay profile of $\text{PVS}^{-\bullet}$ radical into a second order kinetic plot. Results are shown in Table 3. By monitoring the growth and decay profile of the transient absorbances for $\text{PVS}^{-\bullet}$ and for ${}^3\text{ZnP}^{4+*}$ in the absence of PVS, the rate constant for the forward reaction between ${}^3\text{ZnP}^{4+*}$ and PVS (k_f) could be determined by employing a curve fitting program.⁴ By comparing the experimental data with the simulated ones, the value of the forward rate constant that gave the best fit was obtained. These results are also summarized in Table 3.

Discussion:

Spectral changes of ZnP^{4+} in PSS solutions: Changes in the absorption and emission spectra of ZnP^{4+} upon the addition of PSS indicate that a significant interaction between the participating species exists. With the addition of PSS of molecular weight 4,000, having ~ 20 monomer residues per chain the absorbance of ZnP^{4+} at 434 nm decreases (Figure 3) initially up to $P/D = 4$, but as more PSS is titrated into the solution, the absorbance increases up to a plateau at $P/D = 25$ and above. Clearly, the P/D ratio is a very important parameter. These changes can be attributed to binding of the cationic species ZnP^{4+} to the anionic polyelectrolyte, PSS, by electrostatic interaction,¹⁸⁻²³ which produces an inhomogeneous distribution of ZnP^{4+} in solution.²⁴

For PSS of molecular weight 4,000, at $P/D \approx 4$, each macroion can hold five ZnP^{4+} cations. The PSS bound ZnP^{4+} closest to the incoming photon can absorb light and at the same time obstruct one or more of its close lying ZnP^{4+} neighbors on the same polyelectrolyte chain from absorbing photons. This shadowing effect leads to an overall decrease in the apparent extinction coefficient from that observed in aqueous solution in the absence of PSS when the porphyrin is molecularly dispersed.²⁴

When PSS of molecular weight 500,000 is employed, the same shadowing effect is observed at $P/D \leq 4$, but to a greater extent. While with PSS of molecular weight 4,000, only five ZnP^{4+} cations bind at $P/D \approx 4$ to each macromolecule, for PSS of molecular weight 500,000, about 600 ZnP^{4+} cations can bind at the same P/D ratio. Thus, the formation of a larger cluster of ZnP^{4+} cations becomes possible with this high molecular weight PSS macroion, which causes a larger shadowing effect. With this PSS sample, an additional feature becomes apparent, namely, the enhancement of absorbance in the region 448 nm to 550 nm, with well defined isosbestic points. This feature is attributed

to intermolecular interaction of ZnP^{4+} species bound to the same polyelectrolyte chain. The existence of well defined isosbestic points indicates the appearance of a single new absorbing species, probably a dimer. Single photon counting techniques, do, in fact, show a two component fluorescence decay. The minor component ($\sim 40\%$) has the same lifetime as the monomer, 1.4 ns, while the major component ($\sim 60\%$), which we ascribe to the dimer, has a lifetime of 0.5 ns. This shorter lifetime of the dimer is consistent with the findings of others.¹⁷

The chain length of the macroion appears to be very important in the dimerization process. The skeleton of the long chain, 500,000 M.W. PSS is more flexible than that of the 4,000 M.W. one. Because of this increased flexibility the longer chain can bend around and the polymer bound ZnP^{4+} cations can exhibit characteristics of a dimer.

The red-shift of the Soret band maximum with the addition of PSS to an aqueous solution of ZnP^{4+} reflects the existence of a different kind of microenvironment around ZnP^{4+} counterions. At $P/D > 4$, the absorption intensity increases because the ZnP^{4+} cations are progressively sequestered in dispersed form as the monomer in the environment of the polymer. It is very well known that porphyrin spectra are very sensitive to the environment.²⁵⁻²⁸ The red-shift in the spectra of ZnP^{4+} is ascribed to the hydrophobic interaction between ZnP^{4+} and the aromatic moieties on the PSS. The spectrum of ZnP^{4+} in the solution of a monomeric analog of PSS, sodium benzene sulfonate, however, does not exhibit the same spectral change upon the addition of an equivalent amount of PSS. It requires the cooperative effect of the aromatic moieties to produce the environment that causes the red-shift in the PSS solutions. The effect of different solvents on the spectrum of ZnP^{4+} was also studied.²⁹ It was found that for all solvents tested, the Soret band of ZnP^{4+} shifts to longer wavelengths in less polar solvents, e.g., nitrobenzene. This is consistent with the conclusion that hydrophobic interactions of ZnP^{4+} with the aromatic interior of PSS is responsible for the red-shift

in λ_{max} . The pendant aromatic groups together with the alkyl skeleton constitute the hydrophobic environment in PSS. The decrease in fluorescence quantum yield of ZnP^{4+} at $P/D \leq 4$, as Table 1 shows, is consistent with concentration-induced quenching since it is more pronounced with the higher molecular weight PSS (Figure 6).

Influence of PSS on the triplet state lifetimes: Using laser flash techniques the influence of PSS on the triplet lifetime of ZnP^{4+} was investigated. In pure aqueous medium, ${}^3ZnP^{4+*}$, $\lambda_{mon} = 480$ nm, has a lifetime of 3.3 ms. On binding with PSS, M.W. = 4,000 at $P/D = 4$, the lifetime is shortened considerably to 0.44 ms and at $P/D = 25$, the triplet lifetime is 0.83 ms. This lifetime shortening in PSS environment can be ascribed either to the migration of the triplet excitation energy to nearby ZnP^{4+} cations or to triplet-triplet annihilation and subsequent dissipation of the excitation energy as thermal energy as shown in Scheme 1, steps (5) and (6). With PSS of M.W. 500,000, the lifetime is so short that we cannot detect a ${}^3ZnP^{4+*}$. At a P/D ratio of 200 with PSS of 4000 M.W., the lifetime of ${}^3ZnP^{4+*}$, 1.4 ms, is shorter than in pure water, probably because of the difference in the microenvironment.

Photoinduced electron transfer in PSS environment: In order to probe the effect of PSS on the overall quantum efficiency of photoinduced electron transfer reactions between ZnP^{4+} and PVS, steady state photolysis experiments have been performed using triethanolamine as the irreversible electron donor (Table 2). Laser flash studies were also employed to investigate the electron transfer reaction between PVS and ${}^3ZnP^{4+*}$ in the absence of any sacrificial donor (Table 3). The individual steps in the overall process are shown in Scheme 1. The PSS bound ZnP^{4+} species, represented as $P-ZnP^{4+}$, is excited to the first excited singlet state upon the absorption of a photon. Rapid intersystem crossing ($k_{ISC} = 6.4 \times 10^8 \text{ s}^{-1}$)³⁰ occurs to the lowest excited triplet state. ${}^3ZnP^{4+*}$ can undergo unimolecular decay or it can be depleted via collisional quenching with

PVS, energy transfer quenching with residual oxygen or with other impurity quenchers. Alternatively, ${}^3\text{ZnP}^{4+*}$ can also be depleted via mutual annihilation with another PSS bound ${}^3\text{ZnP}^{4+*}$ or via concentration-induced quenching with another neighboring ground state P—ZnP^{4+} . All these energy wasting quenching processes compete with the forward reaction (step 7) by which an electron is transferred from ${}^3\text{ZnP}^{4+*}$ to PVS resulting in the formation of ZnP^{5+*} and PVS^{-*} . Back reaction (step 8) of the initial photoproducts is in competition with the sacrificial donor reaction (step 9).

Back reaction leads to no net PVS^{-*} formation. As Table 3 shows, in pure water, the back reaction rate is three orders of magnitude faster than the rate obtained for a medium containing PSS of M.W. 4000 at P/D ratio of 25. The presence of PSS, however, decreases the forward rate by a factor of 25. The retardation of the back reaction rate can be understood from the ionic repulsion phenomenon as shown in Scheme 2. In the anionic environment of the polyelectrolyte, PVS^{-*} is quickly repelled while ZnP^{5+*} is still retained. Thus the redox products are kept isolated longer than in pure water. Although, this repulsion is expected to be more at P/D = 200 than at 25, a decisive discrepancy exists in favor of P/D = 25. It is probable that at a very high P/D ratio, like 200, the photoproducts are trapped in a cage-like environment and as a result the mobility of the reacting partners is decreased. Consequently, the back reaction and the cage escape process become competitive. Retardation of the forward reaction rate can be explained as follows: In order for the forward reaction to take place, the zwitterionic viologen species has to intercept ${}^3\text{ZnP}^{4+*}$ within the excited state lifetime of the latter. In the PSS environment, ZnP^{4+} remains encapsulated in the polymer matrix because of electrostatic and hydrophobic interactions while PVS experiences no such binding interaction. Therefore, the diffusion of PVS to ${}^3\text{ZnP}^{4+*}$ becomes slow and k_f decreases.

The steady state quantum yields are consistent with the findings from laser flash studies. For PSS of molecular weight 4,000, the quantum yield for PVS^{-*} radical

formation increases from 0.91 in pure water to 1.26 at $P/D = 25$ and to 1.03 at $P/D = 200$. The enhanced values of the radical yield reflect the influence of k_b at the respective P/D ratio. However, at $P/D = 4$, with this PSS sample, $\Phi_{PVS-\bullet}$ is 0.43 and with PSS of M.W. 500,000, $\Phi_{PVS-\bullet}$ is only 0.17 at $P/D = 3.5$. These low values can be explained by the existence of competitive pathways for the destruction of ${}^3ZnP^{4+}$. Under steady state illumination conditions, concentration-induced quenching of the ${}^3ZnP^{4+}$ species (step 6, Scheme 1) can compete with the forward electron transfer step (Step 7). The overall high efficiency in generating $PVS^{-\bullet}$ radical primarily stems from the fact that our photosensitizer has a very high triplet yield ($\sim 90\%$).³⁰ Having a quantum efficiency of greater than unity is not uncommon when one of the decomposition products of the sacrificial donor maintains some reducing power. This has been adequately explained in literature.³¹

Conclusion:

The present study highlights the importance of P/D ratios in interfacial phenomena involving polyelectrolytes. From flash photolysis and steady state studies it appears that there is an optimum P/D ratio where a maximum quantum storage is achieved. In our present study with PSS of 4,000 M.W., this optimum P/D ratio is 25. At a very low P/D ratio ($P/D \leq 4$) intermolecular interactions of the polyelectrolyte bound species exist and the net quantum storage in the form of $PVS^{-\bullet}$ radical is poor. At a very high P/D ratio, $P/D \geq 200$, because of the hydrophobic envelopment of the photosensitizer, the forward electron transfer rate is hindered. With the PSS of molecular weight 500,000 we have not reached the optimum value of the P/D ratio for highest quantum yield.

While our study with only one polyelectrolyte, PSS, does not firmly establish the generality of the importance of P/D ratios in electron transfer efficiency, it suggests future work in which the role of P/D ratio and chain-length should be explored for the desired optimization of photoinduced electron transfer yield.

Acknowledgement: The work described in this paper was supported by the Office of Energy Research, Office of Basic Energy Sciences, Chemical Sciences Division of the U.S. Department of Energy under contract No. DE-AC03-76SF00098.

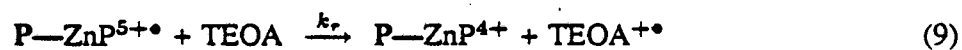
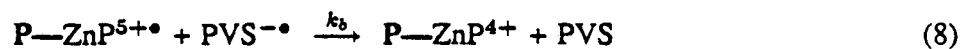
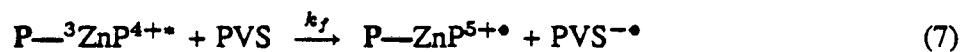
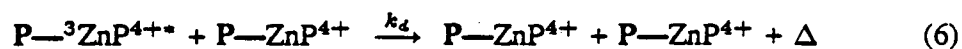
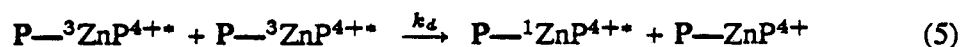
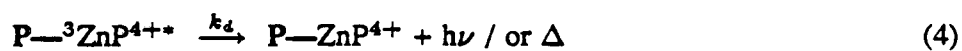
REFERENCES

1. Willner, I.; Otvos, J. W.; Calvin, M. *J. Am. Chem. Soc.* **1981**, *103*, 3203.
2. Willner, I.; Yang, J-M; Laane, C.; Otvos, J. W.; Calvin, M. *J. Phys. Chem.* **1981**, *85*, 3277.
3. Laane, C.; Willner, I.; Otvos, J. W.; Calvin, M. *Proc. Nat. Acad. Sci. USA* **1981**, *78*, 5928.
4. Otvos, J. W.; Casti, T. E.; Calvin, M. *Sci. Pap. Inst. Phys. Chem. Res. (Jpn.)*, **1984**, *78*, 129 (English).
5. Whitten, D. G.; Russel, J. C.; Schmehl, R. H. *Tetrahedron* **1982**, *38*, 2455.
6. Meisel, D.; Matheson, M. S. *J. Am. Chem. Soc.* **1977**, *99*, 6577.
7. Brugger, P. -A.; Gratzel, M. *J. Am. Chem. Soc.* **1980**, *102*, 2461.
8. Sassoon, R. E.; Gershuni, S.; Rabani, J. *J. Phys. Chem.* **1985**, *85*, 1937.
9. Itoh, Y.; Morishima, Y.; Nozakura, S. *Photochem. Photobiol.* **1984**, *39*, 451.
10. Nagamura, T.; Takeyama, N.; Tanaka, K.; Matsuo, T. *J. Phys. Chem.* **1986**, *90*, 2247.
11. Meyerstein, D.; Rabani, J.; Matheson, M. S.; Meisel, D. *J. Phys. Chem.* **1978**, *82*, 1879.
12. (a) Morishima, Y.; Itoh, Y.; Nozakura, S.; Ohno, T.; Kato, S. *Macromolecules*, **1984**, *17*, 2264.

- (b) Okubo, T.; Turro, N. J. *J. Phys. Chem.* **1981**, *85*, 4034.
(c) Turro, N. J.; Okubo, T. *J. Phys. Chem.* **1982**, *86*, 1535.
13. Jones, G., II.; Goswami, K.; Halpern, A. M. *Nouv. J. Chim.* **1985**, *9*, 647.
14. Parker, C. A.; Rees, W. T. *Analyst*, **1969**, *85*, 587.
15. Demas, J. N.; Crosby, G. A. *J. Phys. Chem.* **1971**, *75*, 991.
16. Calvert, J. G.; Pitts Jr., J. N. *Photochemistry* (Wiley, New York), **1966**, PP 784.
17. (a) Brookfield, R. L.; Ellul, H.; Harriman, A. *J. Chem. Soc., Faraday Trans. 2*, **1985**, *81*, 1837.
(b) Yuzhakov, V. I. *Russ. Chem. Rev.* **1979**, *48*, 1076.
(c) Perrin, J. *Ann. Phys.* **1932**, *17*, 283.
(d) Förster, T. *Ann. Phys.* **1948**, *32*, 55.
(e) Zweig, A.; Huffman, K. R. *J. Am. Chem. Soc.* **1974**, *96*, 1449.
18. Crescenzi, V.; Quadrifoglio, F.; Vitagliano, V. *J. Macromol. Sci. (Chem)*. **1967**, *A1(5)*, 917.
19. (a) Yamaoka, K.; Takatsuki, M. *Bull. Chem. Soc. Jpn.* **1978**, *51*, 3182.
(b) Takatsuki, M.; Yamaoka, K. *Bull. Chem. Soc. Jpn.* **1979**, *52*, 1003.
20. Lifson, S. *J. Chem. Phys.* **1964**, *40*, 3705.
21. Shirai, M.; Nagatsuka, T.; Tanaka, M. *Makromol. Chem.* **1977**, *178*, 37.
22. Takatsuki, M. *Bull. Chem. Soc. Jpn.* **1980**, *53*, 1922.
23. Yamaoka, K.; Matsuda, T.; Murakami, T. *Bull. Chem. Soc. Jpn.* **1981**, *54*, 3859.

24. Orvos, J. W.; Stone, H.; Harp Jr., W. R. *Spectrochim. Acta*, **1957**, *9*, 148.
25. Pasternack, R. F.; Spire, E. G.; Teach, M. *J. Inorg. Nucl. Chem.* **1974**, *36*, 599.
26. (a) Barry, C. D.; Hill, H. A. O.; Mann, B. E.; Sadler, P. J.; Williams, R. J. P. *J. Am. Chem. Soc.* **1973**, *95*, 4545.
(b) Mauzerall, D.; *Biochemistry*, **1965**, *4*, 1801.
27. Pasternack, R. F. *J. Am. Chem. Soc.* **1972**, *94*, 4511.
28. Seely, G. R.; Jensen, R. G. *Spectrochimica Acta*, **1966**, *21*, 1835.
29. Casti, T. E.; *Dissertation*, **1985**, (University of California, Berkeley, CA 94720)
30. Harriman, A.; Porter, G.; Richoux, M. *J. Chem. Soc., Faraday Trans. 2* **1981**, *77*, 833.
31. Chan, S. F.; Chou, M.; Creutz, C.; Matsubara, T.; Sutin, N. *J. Am. Chem. Soc.* **1981**, *103*, 369.

SCHEME 1



* P represents poly(styrene sulfonate) (PSS).

SCHEME 2

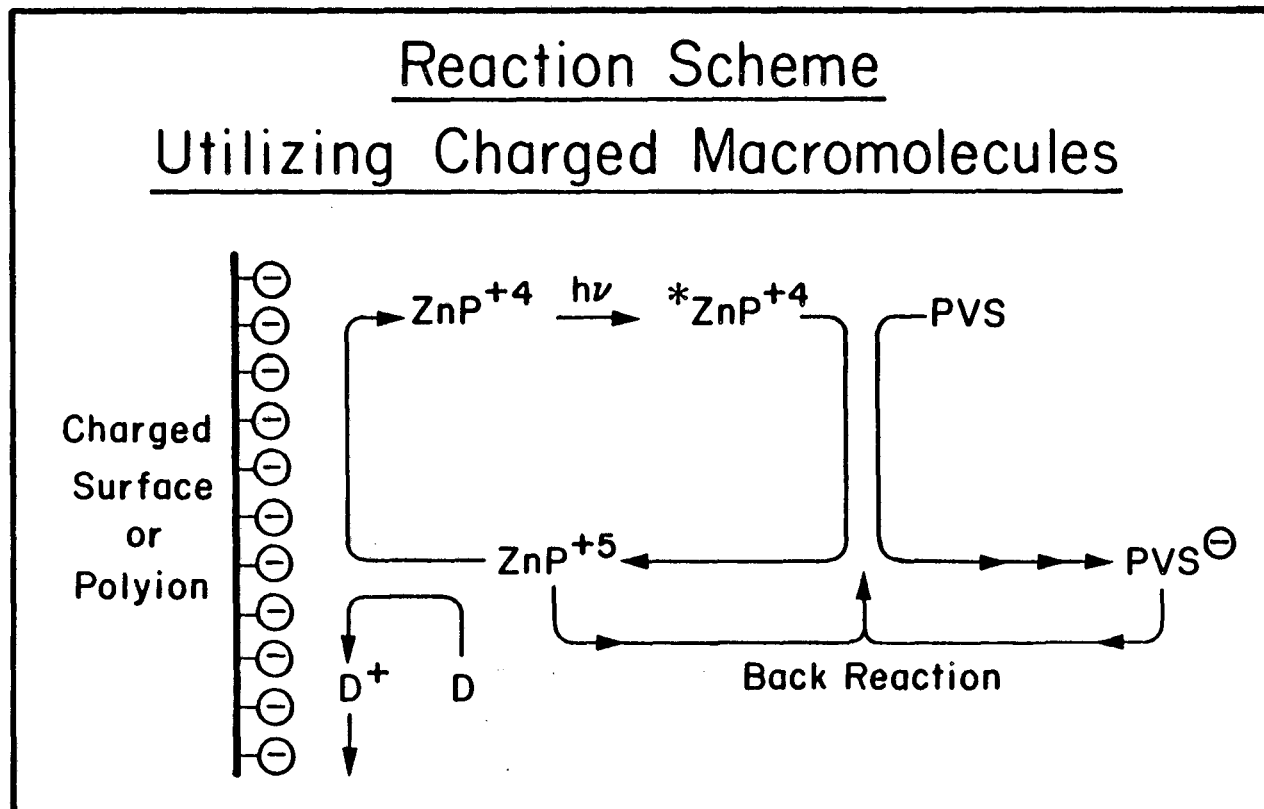


TABLE 1

PHOTOPHYSICAL PARAMETERS ASSOCIATED WITH
THE SORET BAND OF ZnP^{4+}

Medium	λ_{abs} (nm)	λ_{flr} (nm)	Φ_{flr}	τ_S (ns)	τ_T (ms)
Water	434	630	0.031	1.4	3.30
PSS (4k, P/D = 4)	438	625	0.025	—	0.44
PSS (4k, P/D = 25)	442	623	0.038	—	0.83
PSS (4k, P/D = 200)	442	623	0.040	1.6	1.40
PSS (500k, P/D = 3.5)	438	630	0.006	0.5 1.4	—
PSS (500k, P/D = 25)	440	625	0.016	—	—

TABLE 2

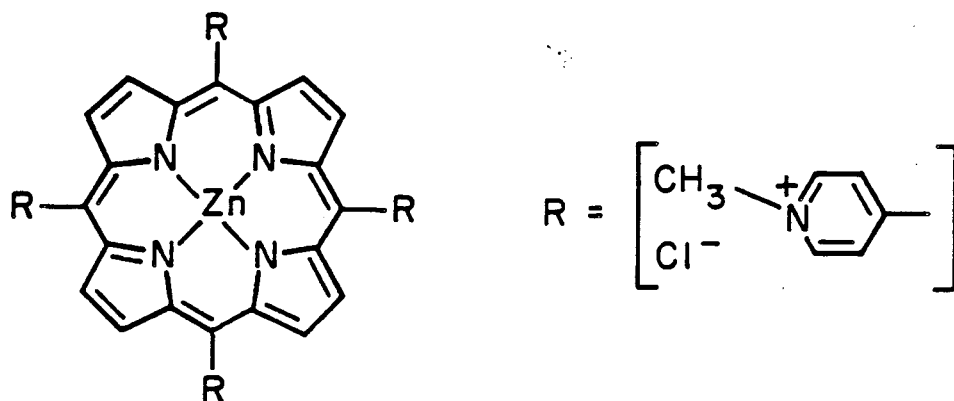
PHOTOINDUCED ELECTRON TRANSFER REACTION
RESULTS ON STEADY STATE QUANTUM YIELDS

Medium	Donor	pH	Φ
Water	TEOA	10.0	0.91
PSS (4k, P/D = 4)	TEOA	10.0	0.43
PSS (4k, P/D = 25)	TEOA	10.0	1.26
PSS (4k, P/D = 200)	TEOA	10.0	1.03
PSS (500k, P/D = 3.5)	TEOA	10.0	0.19
PSS (500k, P/D = 200)	TEOA	10.0	1.08

TABLE 3

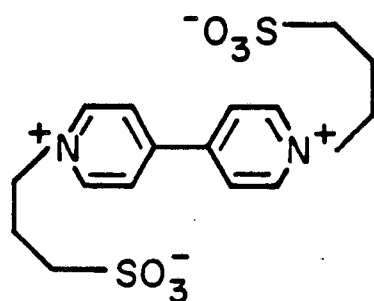
LASER FLASH PHOTOLYSIS DATA

Medium	$10^{-5} \times k_f$ $M^{-1} s^{-1}$	$10^{-6} \times k_b$ $M^{-1} s^{-1}$
Water	300	6500
PSS (4k, P/D = 25)	12.0	6.4
PSS (4k, P/D = 200)	6.5	160



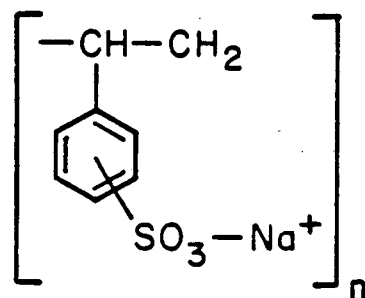
$$\text{ZnP}^{+4}$$

Zinc *meso*-tetra(4-N-methyl pyridinium) Porphyrin



PVS

Propyl Viologen Sulfonate



PSS

Poly(styrene sulfonate)

FIGURE CAPTIONS

Figure 1. Absorption spectrum of ZnP^{4+} (5.0×10^{-6} M) in pure water.

Figure 2. Emission and excitation spectra of ZnP^{4+} (5.0×10^{-6} M) in pure water (intensity in arbitrary units).

Figure 3. Absorption spectra of ZnP^{4+} (5.0×10^{-6} M) in the presence of poly(styrene sulfonate) (M. W. = 4k) in aqueous medium at various P/D ratios; the curves in descending order with respect to the absorption peak at 434 nm, represent P/D = 0, 2 and 4. The dashed curve represents P/D = 25.

Figure 4. Absorption spectra of ZnP^{4+} (5.0×10^{-6} M) in the presence of poly(styrene sulfonate) (M. W. = 500k) in aqueous medium at various P/D ratios; the curves in the descending order with respect to the absorption at 434 nm, represent P/D = 0, 0.5, 1, 1.5, 2, 3 and 3.5. The dashed curve represents P/D = 25.

Figure 5. Variation of the absorbance at 434 nm for ZnP^{4+} in the presence of poly(styrene sulfonate) as a function of P/D ratio.

Figure 6. Emission spectra of ZnP^{4+} (5.0×10^{-6} M) bound to poly(styrene sulfonate) at various P/D ratios (intensity in arbitrary units, $\lambda_{exc} = 448$ nm). (a) in pure water, (b) P/D = 4 (4k PSS), (c) P/D = 25 (4k PSS), (d) P/D = 3.5 (500k PSS) and (e) P/D = 25 (500k PSS).

Figure 1

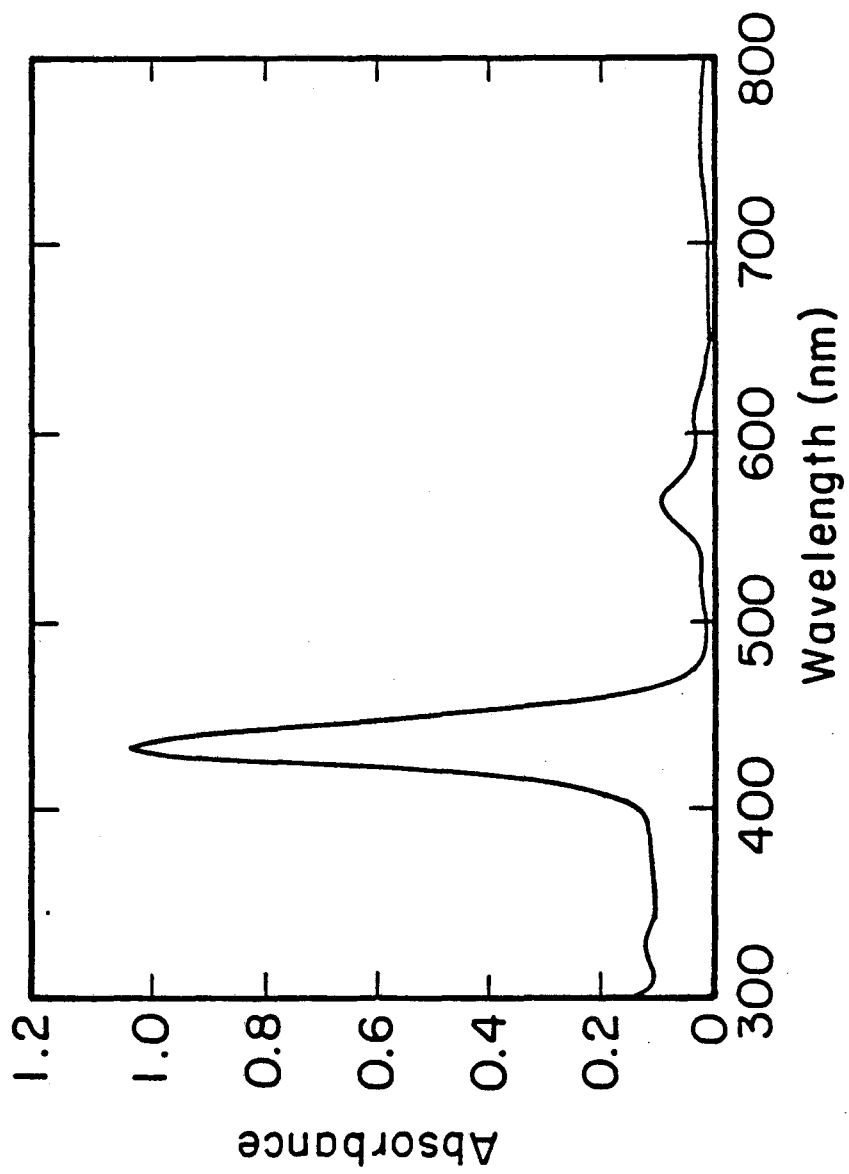
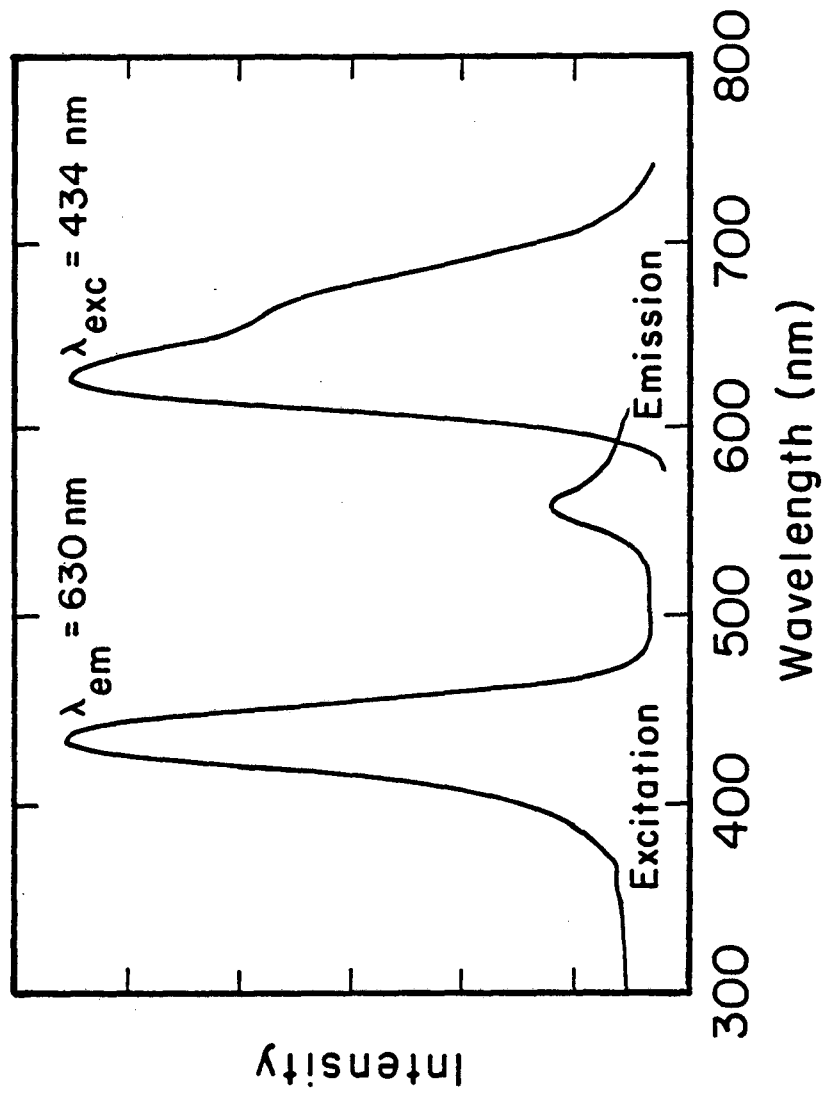
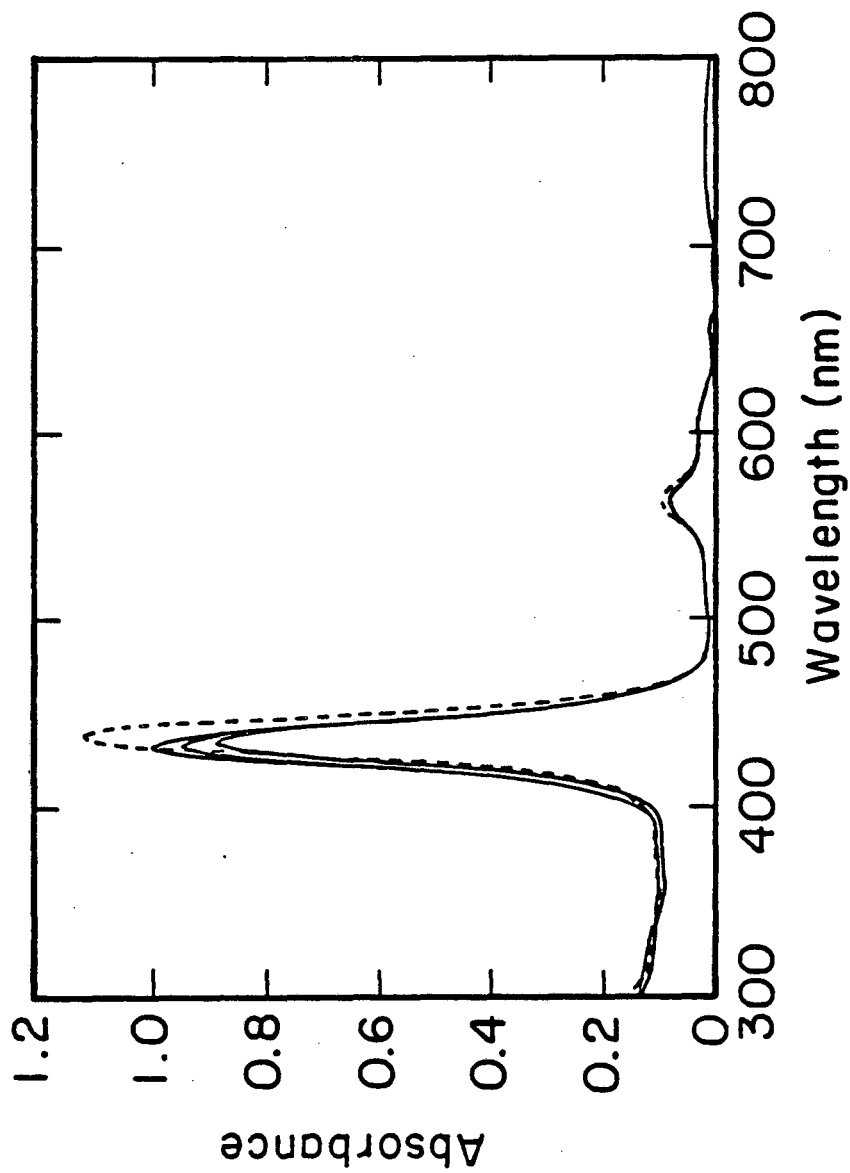


Figure 2





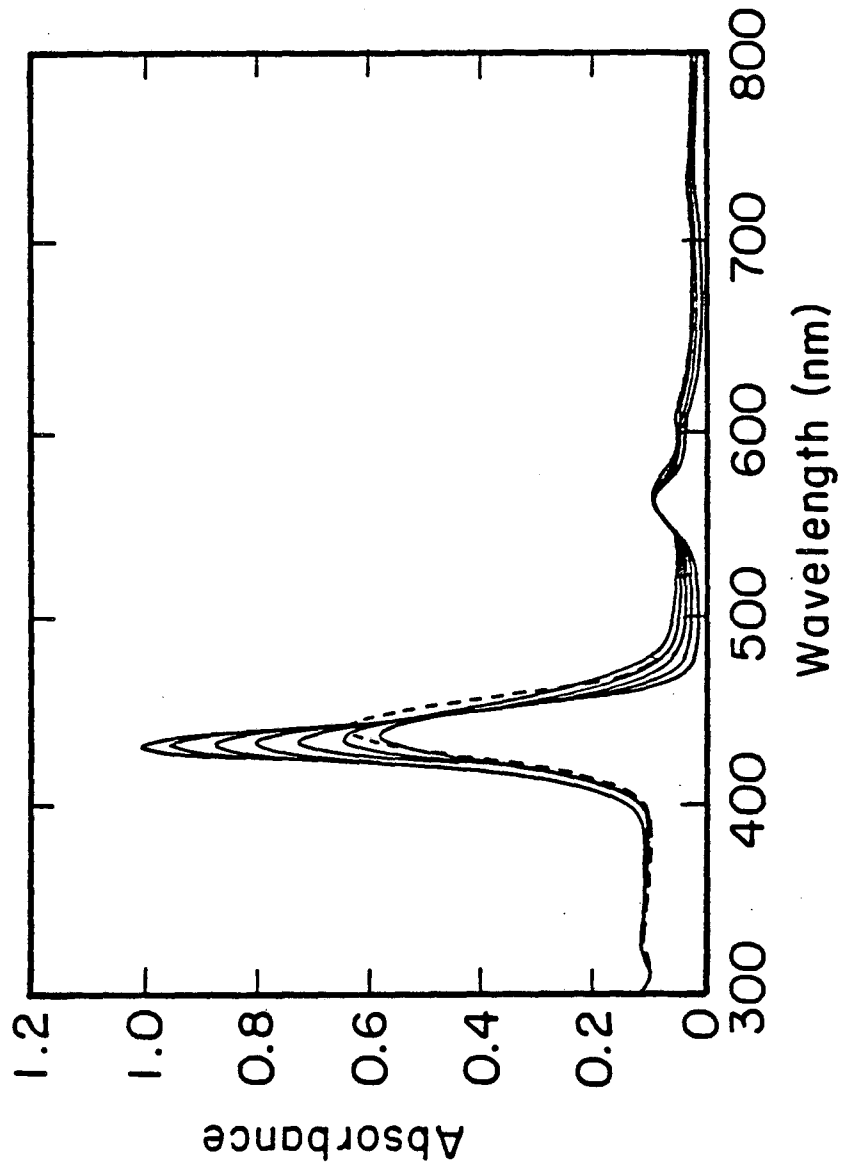


Figure 5

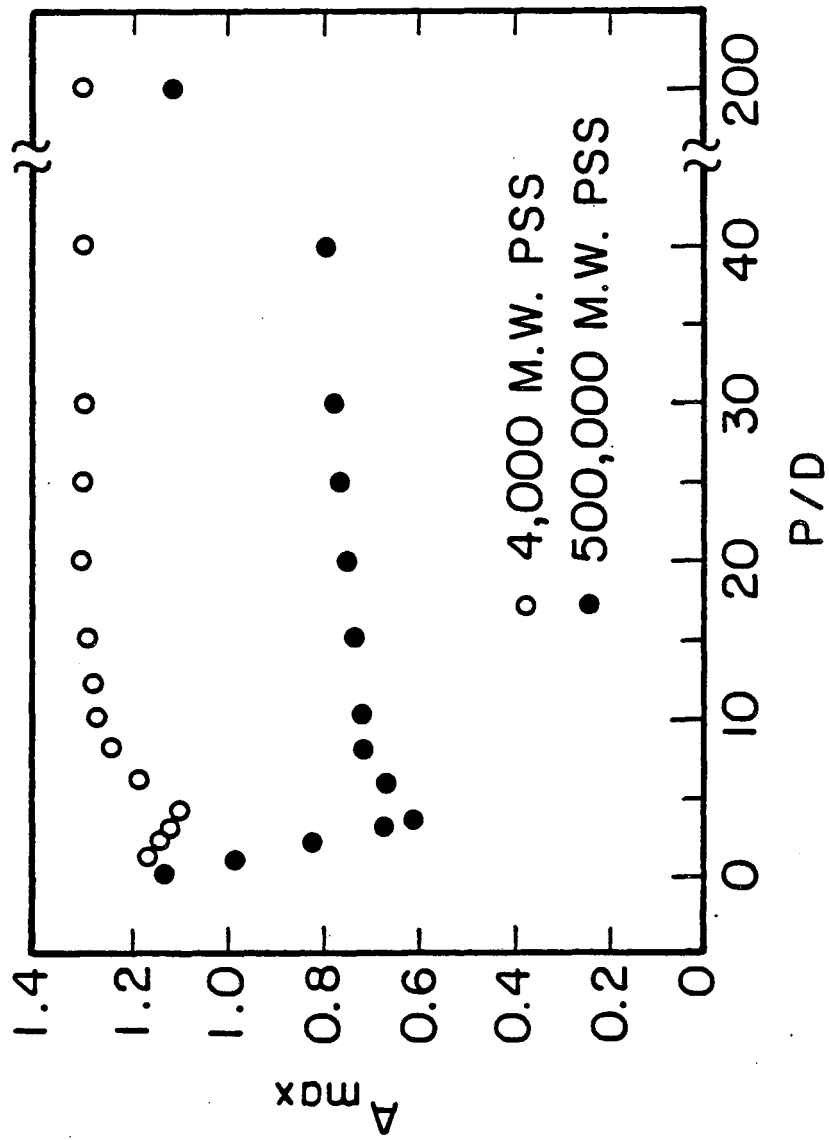
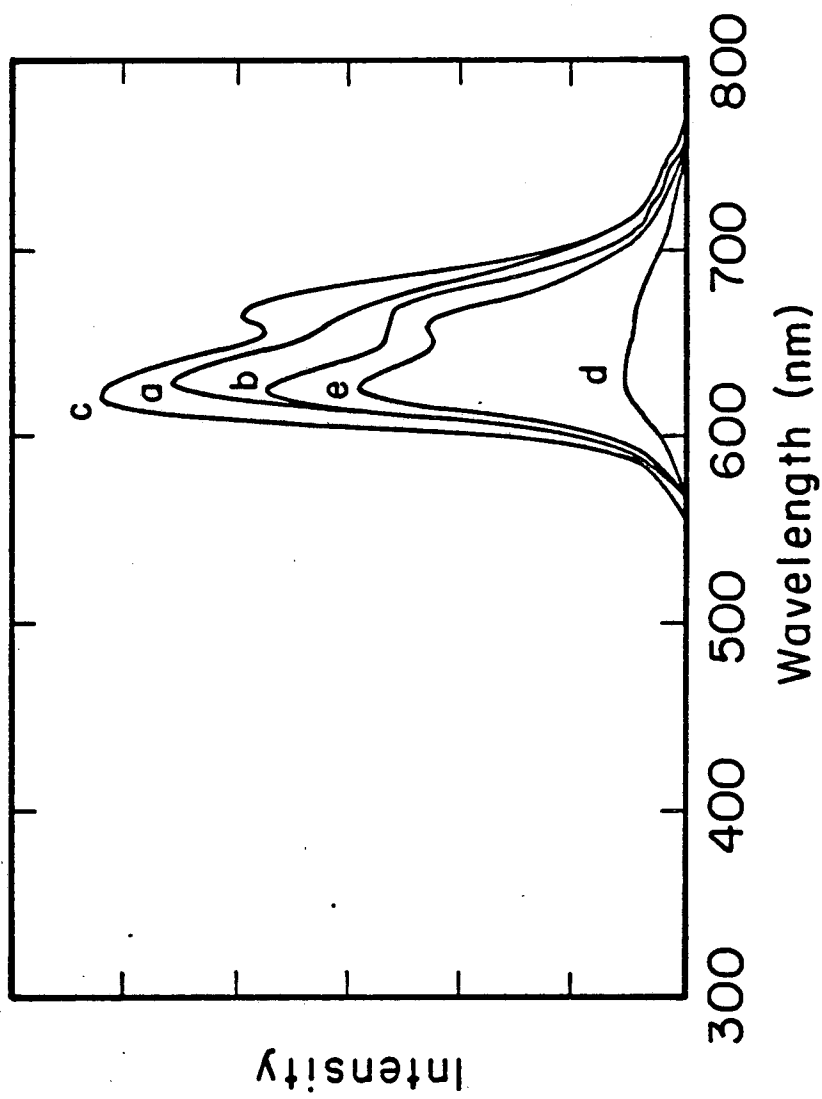


Figure 6



This report was done with support from the Department of Energy. Any conclusions or opinions expressed in this report represent solely those of the author(s) and not necessarily those of The Regents of the University of California, the Lawrence Berkeley Laboratory or the Department of Energy.

Reference to a company or product name does not imply approval or recommendation of the product by the University of California or the U.S. Department of Energy to the exclusion of others that may be suitable.

TECHNICAL INFORMATION DEPARTMENT
LAWRENCE BERKELEY LABORATORY
UNIVERSITY OF CALIFORNIA
BERKELEY, CALIFORNIA 94720